



**HAL**  
open science

## Ultra-Low-Power Logic with Contactless Capacitive MEMS

Aleksandra Markovic, Laurent Mazonq, Adrian Laborde, Herve Fanet, Gael Pillonnet, Bernard Legrand

► **To cite this version:**

Aleksandra Markovic, Laurent Mazonq, Adrian Laborde, Herve Fanet, Gael Pillonnet, et al.. Ultra-Low-Power Logic with Contactless Capacitive MEMS. 21st International Conference on Micro and Nanotechnology for Power Generation and Energy Conversion Applications (PowerMEMS 2022), Dec 2022, Salt Lake City, United States. pp.233-227, 10.1109/PowerMEMS56853.2022.10007572 . hal-03946985

**HAL Id: hal-03946985**

**<https://hal.science/hal-03946985v1>**

Submitted on 19 Apr 2023

**HAL** is a multi-disciplinary open access archive for the deposit and dissemination of scientific research documents, whether they are published or not. The documents may come from teaching and research institutions in France or abroad, or from public or private research centers.

L'archive ouverte pluridisciplinaire **HAL**, est destinée au dépôt et à la diffusion de documents scientifiques de niveau recherche, publiés ou non, émanant des établissements d'enseignement et de recherche français ou étrangers, des laboratoires publics ou privés.

# ULTRA-LOW-POWER LOGIC WITH CONTACTLESS CAPACITIVE MEMS

*Aleksandra Marković<sup>1</sup>, Laurent Mazon<sup>1</sup>, Adrian Laborde<sup>1</sup>, Hervé Fanet<sup>2</sup>,  
Gaël Pillonnet<sup>2</sup> and Bernard Legrand<sup>1</sup>*

<sup>1</sup> LAAS, Univ. Toulouse, CNRS, Toulouse, France and

<sup>2</sup> Univ. Grenoble Alpes, CEA LETI, Grenoble, France

## ABSTRACT

We report the simulation, design, fabrication and performance assessment of capacitive MEMS, carrying out contactless electromechanical computing with ultra-low-power consumption. The novel concept is implemented on silicon using on-purpose differential comb-drive actuators. This shift in the paradigm allows near-zero power dissipation by asymptotically suppressing static and dynamic energy losses which are inherently present in current hardware for logic implementation. Furthermore, this novel approach based on capacitive information encoding allows recovery of the invested charges by the power supply asymptotically suppressing dynamic losses and opening the way towards adiabatic operation. At the very least, the contactless operation resolves the reliability issues in existing electromechanical logics based on N/MEMS relays.

## KEYWORDS

MEMS, logic states, comb-drive actuators.

## INTRODUCTION

The energy dissipation of the state-of-the-art CMOS-based logic gates is limited by the inherent trade-off between dynamic and static losses which are due to abrupt switching (energy dissipation is proportional to  $CV^2$ ) and leakage currents in the transistors, respectively [1]. Dynamic losses can obviously be reduced by lowering the power supply as in sub-threshold logic systems but with limitation coming from subthreshold slope of any field-effect transistor. In practice,  $1000 k_B T$  dissipation is achieved in recent CMOS logics. Moreover, the bottom limit in non-adiabatic logic is also governed by the thermal noise. Simply put, in order to distinguish between the two states - “0” and “1”, the minimum invested energy has to be at least  $100 k_B T$ . Dynamic dissipation can be further reduced by using energy recycling logic, so called adiabatic. By using a reversible power source (power-clock PC) to supply the devices it is possible to recover the charges that are invested in the logic state encoding. Dissipation in the adiabatic logic is governed by the slope of the power clock signal. By decreasing the PC slope, we can reduce the energy dissipated during the state switching, that is dynamic energy. However, the static losses remain present. Moreover, the static dissipation becomes dominant as the logic operation decreases. The tradeoff between minimizing static and dynamic losses is therefore necessary, but the energy gain is limited due to finite transistor I/V subthreshold slope. Some previous works in the field have made use of nano/micro-electro-mechanical system (N/MEMS) relays to overcome this inherent tradeoff concerning FETs [3-5]. In the “off” state relays break the connection between the power source and the ground and therefore avoid leakage currents. However,

they have comparably large dimensions, blurry “ON”-state contacts and poor mechanical reliability for the high amount of switching that is required in a digital system.

Here, we propose an approach enabling the coding of logic states in the displacement of capacitive and contactless MEMS for the purpose of ultra-low-power electromechanical processing of information, based on [1-2]. Contactless operation eliminates losses due to leakage currents and mechanical non-reversibility while increasing robustness of the devices. Capacitive transduction allows recovering of the invested electromechanical energy through charge transfer with the power supply. This theoretically makes the whole operation dissipation-free if the speed is slowed down accordingly. Residual energy losses actually arise from mechanical dissipation in materials and air and from residual dynamic loss (scaled down linearly with logic operation frequency) according to the well-known adiabatic operations [6]. Therefore, the energy dissipated per logic operation is reduced orders of magnitude below the dynamic losses in CMOS gates, justifying the adiabatic promises.

In the following sections we show the behavior modelling of the differential comb-drive actuators that was based on the FEM simulations. We show the benefits of the unconventional operation of comb-drives (with no initial finger coverage) and that the contribution of the fringing fields can be exploited to lower down the dissipation during the logic state computation. Finally, we report the fabrication of the MEMS device capable of representing logic states and demonstrate its functioning in a quasi-static operation.

## DESIGN AND SIMULATIONS

Our proposed device consists of micromechanical devices with moveable subparts, in particular comb-drive actuators, and transmits logic state through the gate by displacement. Depending on the position of the device, capacitance between the interdigitated combs changes – providing the information that can further be electromechanically processed and converted into a voltage logic state thanks to a variable capacitive divider formed by the MEMS output capacitance and a fixed comb-drive.

To maximize the robustness, the gate operates in dual rail logic requiring the input state A and the opposite state  $A_b$ . Two comb-pairs are connected to the differential inputs A,  $A_b$ . To maximize the level of logic differentiation the comb is not overlapped in resting condition (when  $A=A_b$ ). The input voltages are risen smoothly according to the adiabatic operation.

Comb-capacitors have been extensively analyzed and modelled [7][8] when the combs are well covered, but there is a lack of previous studies in the zero-overlap regime. As the purpose of this work requires the operation of MEMS

comb-drives in this unconventional configuration, experiment and FEM simulations are required to better know the variation of capacitance and generated force in the proximity of the no-overlap i.e. when the displacement around the resting position is of the order of magnitude of the finger-gap value  $d$ . Unlike the energy harvesting and sensing comb-drive systems, which aim at maximizing the amount of charges induced by the movement, our aim is to reduce the amount of charge invested in the comb-drive while maximizing the displacement.

Fig.1 shows the illustration of a single comb-pair whose comb coverage  $x$  was varied from very negative ( $\gg$  gap width  $d$ ) to the closed gap (full finger coverage). We found an analytical model that fit the individual FEM values of the mutual capacitance within the comb-drive (excluding parasitic contributions).

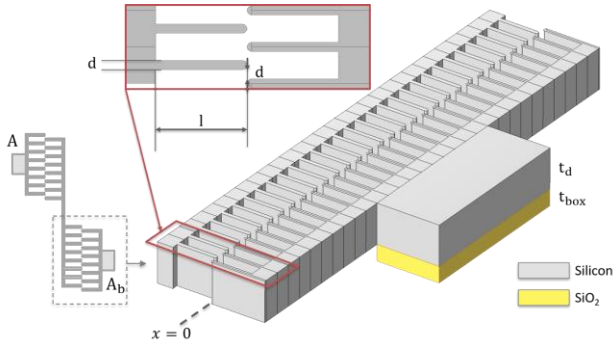


Figure 1: Schematic of a single comb-drive actuator with  $t_d$  being the thickness of the device,  $t_{box}$  the thickness of buried oxide,  $l$  the length of the fingers,  $d$  their width as well as the gap between them and  $x$  being the overlap between the combs.

Figure 2 shows the variation of the capacity (normalized to  $C_0 = \epsilon_0 t_d$ ) of a single finger pair in a comb-drive according to the movement of the mobile structure. It is zero when the displacement is very negative, linear for high displacements and of a form between the two that was to be found.

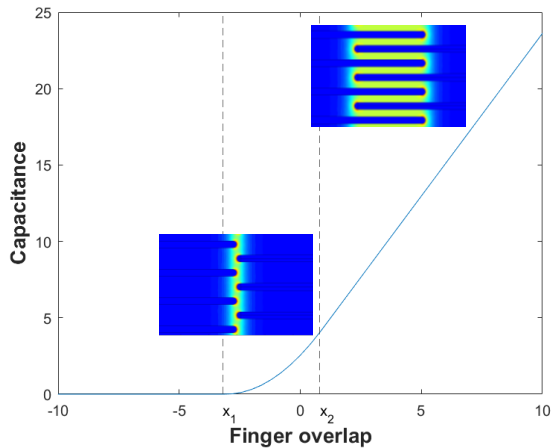


Figure 2: Variation of the mutual capacitance (excluding parasitic capacitance) of a single finger pair with respect to the overlap between the comb-drive fingers. Finger overlap is normalized with the value of the gap  $d$ .

The fitting function as well as its derivative have to be

continuous in order to avoid any discontinuity of the force. This gives us a set of equations and boundary conditions at points  $x_1$  and  $x_2$  that correspond to the transition points between the three regions and that were obtained from the simulations. Solving of the equations gives us the following model for the capacitance variation with regards to the overlap between interdigitated fingers  $x$ :

$$\begin{aligned} x < x_1 & C = 0 \\ x_1 < x < x_2 & C = 0.53 \cdot 10^6 \cdot d \left( x + \frac{1.6 \cdot 10^{-6}}{d} \right)^2 \\ x_2 < x & C = 2.12 \cdot \left( x + \frac{0.6 \cdot 10^{-6}}{d} \right) \end{aligned} \quad (1)$$

With  $\epsilon_0$  being the vacuum permittivity,  $t_d$  the thickness of the device, and  $d$  the width of the finger in the comb-drive, as well as the gap between the interdigitated fingers. The values of  $x_1$  and  $x_2$  are -3.2 and 0.8, respectively, normalized to the gap  $d$ .

FEM simulations have interestingly shown that the extension of this intermediate region depends only on the length of the fingers, of all the geometrical parameters. The simulations also show that the capacitance derivative is almost linear in the intermediate region ( $x_1 < x < x_2$ ) that we will further refer to as gray zone (Fig.3). The operation of the actuators in this gray-zone regime is unconventional, but it appears that a capacitive gradient proportional to the electrostatic force exists even for a negative overlap, due to fringing fields.

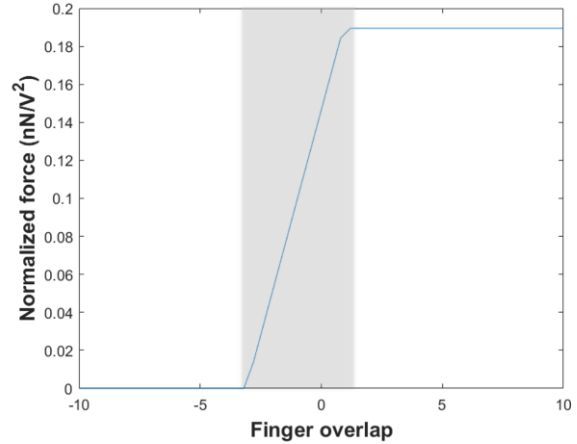


Figure 3: Variation of the normalized force between opposite fingers in a single finger pair with respect to the overlap within the comb-drive. Finger overlap is normalized with the value of the gap  $d$ , force is normalized with the voltage of the power source.

Fig.4 shows the induced displacement of the moveable part per amount of invested charges, depending on the value of the initial overlap of the fingers within the comb-drive. Operation in the range close to zero-initial overlap can result in a  $>40\%$  larger displacement for the same amount of invested charges than the usual operation with the coverage of 50% of the finger length. This is beneficial for the present application as it allows reduction of the energy invested in the logic operation while maintaining the mechanical force required for coding of the logic state in the MEMS displacement and consequently ensuring logic differentiation.

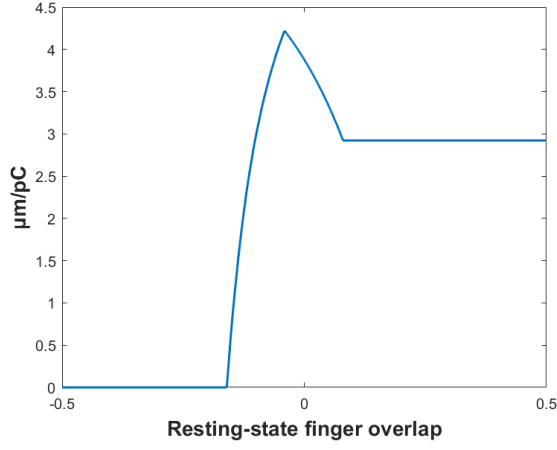


Figure 4: Induced displacement per invested amount of charges for different initial coverage of the combs. Finger overlap is normalized with the length of the fingers.

Modelling of the capacitance and consecutively the force allowed us to observe the relationship between the energy and the logic operation. Fig.5 shows the potential energy of the MEMS mobile part for different sets of applied voltages.

$$E_p = -\frac{C(x)V_A^2}{2} - \frac{C(-x)V_{A_b}^2}{2} + \frac{kx^2}{2} \quad (2)$$

Where  $C(x)$  and  $C(-x)$  are mutual capacitances corresponding to the displacement  $x$  in the comb-pairs, A and  $A_b$  caused by applied voltages  $V_A$  and  $V_{A_b}$ , respectively. The third term represents the mechanical energy of the spring, where  $k$  is the spring constant. In Fig.5, different energy curves represent the potential energy of the moveable part for a given set of applied voltages. Minimum values of the curves correspond to the stable equilibrium positions for each set of  $V_A$  and  $V_{A_b}$  and are indicated in Table 1, where  $V_H$  and  $V_L$  are high and low signal voltages.

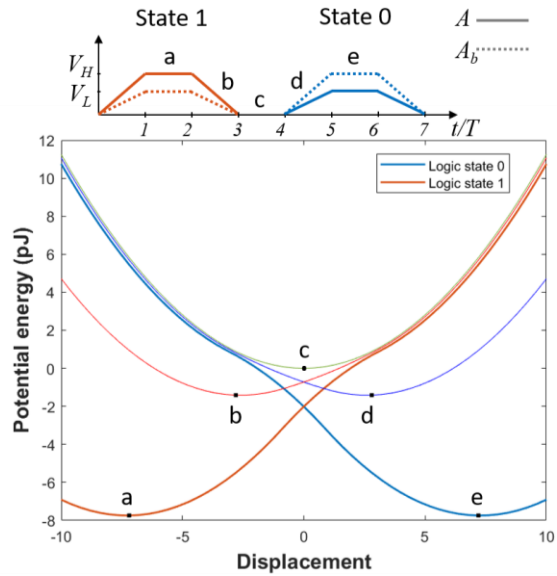


Figure 5: Potential energy of the MEMS moveable part for a given set of voltages applied to the comb-pairs A and  $A_b$ . Minimum values of the curves correspond to the stable equilibrium positions of the moveable MEMS part, relative to the resting position (when applied voltages equal zero).

Table 1: Values of the voltages  $V_A$  and  $V_{A_b}$  in different phases of the transitioning between the two logic states.

	a	b	c	d	e
$V_A$	$V_H$	$V_H/2$	0	$V_L/2$	$V_L$
$V_{A_b}$	$V_L$	$V_L/2$	0	$V_H/2$	$V_H$

Transitioning between the two states includes gradual lowering of the applied signals to zero. In quasi static case, signal ramping time is far below device's resonant frequency to ensure the adiabatic operation. The displacement of the moveable combs lowers towards the resting position, corresponding to the minimum of the potential energy of the comb-pair.

Looking at the energy that is invested in the state encoding (Fig.6) which can be expressed with Eq. 3, at the same state-transition positions as the ones indicated in Table 1, we can see that the change of the invested energy during the adiabatic operation (indicated with a green line) follows a smooth trajectory, minimizing the dissipation.

$$E_{in} = \frac{C(x)V_A^2}{2} + \frac{C(-x)V_{A_b}^2}{2} + \frac{kx^2}{2} \quad (3)$$

The abrupt switching on the other hand (indicated with a black line) causes an energy dissipation of a few tens of pJ during a single operation.

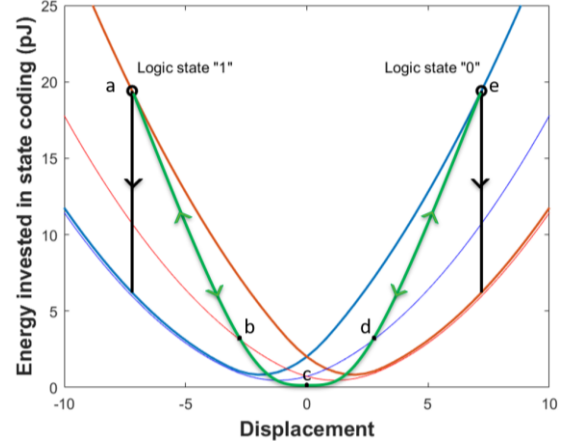


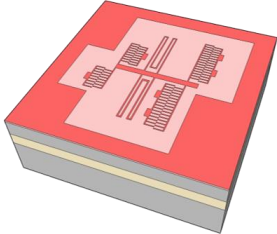
Figure 6: Energy invested in the encoding of the two logic states: 1 (red) and 0 (blue). Quasi-static moving between the logic states ensures non-hysteretic energy exchange between MEMS and the power supply (green curve). Abrupt switching involves inevitable energy losses (black curves).

The energy curves from Fig.5 and Fig.6 correspond to the device as depicted in the fabrication section below.

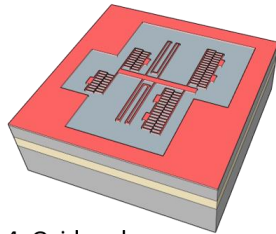
## DEVICE FABRICATION

As the devices include moveable parts, they require fabrication on silicon-on-insulator (SOI) wafers, the buried oxide layer being used as the sacrificial layer during the releasing step. The 4" wafers used are (100) As doped (n-type) wafers with a device layer of  $5\mu\text{m}$  and a buried oxide layer of  $2\mu\text{m}$ . The device layer is highly doped with a resistivity of  $0.001\text{-}0.005\ \Omega\text{cm}$ . The main fabrication steps are shown in the Fig.7.

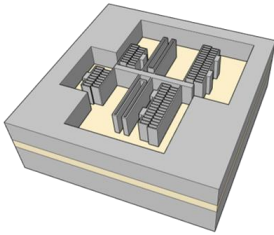
1. Resist exposure



2. Resist development



3. DRIE



4. Oxide release

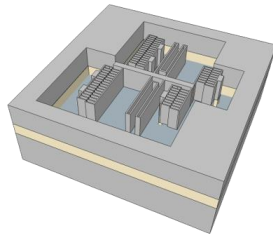


Figure 7: Microfabrication steps: 1. Photoresist exposure, 2. Photoresist development; 3. Deep Reactive Ion Etching, 4. Oxide release in Hydrofluoric Acid.

Before the beginning of the fabrication wafers are cleaned in the standard RCA procedure. This step ensures removal of all the organic and ionic contaminants from the wafer surfaces. Cleaned wafers are first coated with bottom anti reflective coating (BARC) and then with positive photoresist. Pattern is then exposed and developed forming a soft mask. Pattern transfer into the top silicon is performed in a deep reactive ion etching (DRIE) process. Moveable parts are finally released in the hydrofluoric acid that etches the buried oxide beneath the structures. Fig.8 shows the SEM image of a fully fabricated device.

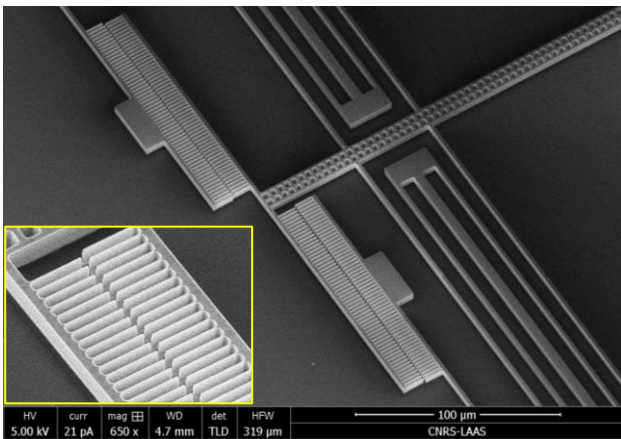


Figure 8: SEM image of the fabricated MEMS device based on comb-drive actuators and capable of representation of logic information, with a zoom-in on fingers within a single actuator. Comb-finger width is  $500\ \text{nm}$ .

Devices were successfully activated, causing lateral movement in the direction governed by the activation voltage (Fig.9).

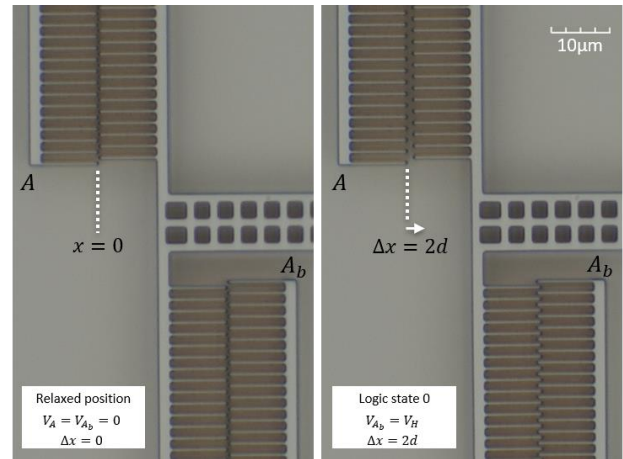


Figure 9: Coding of the logic states in the physical position of the moveable comb (in the value of the mutual capacitance) – relaxed position (left) and logic state 0 (right).

Experimental results are consistent with analytical calculations. Application of a “high” signal to the comb-pair A and “low” to the comb-pair  $A_b$  resulted in a displacement of the moveable part to the left (logic state “1”). Reversing the signals caused to the displacement of the moveable part towards right (logic state “0”).

## CONCLUSION

We have analyzed and modelled a MEMS device capable of performing mechanical coding of the logic information. We have shown that the fringing fields can provide conditions that can be exploited for the purpose of adiabatic computation if the comb-drives are operated in an unconventional configuration, that is with no finger coverage. Moreover, this regime allows us to minimize the charge invested while maximizing the displacement and therefore logic differentiation, which is the opposite goal from the well-known comb-drive actuators used for harvesting or sensing applications. As within our device there is no connection between the power supply and the ground there is no leakage. Capacitive encoding allows for the low amount of invested charges to be further recovered from the comb-drive capacitor by the power supply. Logic state encoded in a mechanical displacement can further be electromechanically processed by additional capacitive MEMS devices, as proposed in [1-2].

## ACKNOWLEDGEMENTS

This work was supported by the French National Research Agency (ANR) under the research project ZerÔuate (grant ANR-19-CE24-0013) and by the RENATECH French national technological network.

## REFERENCES

- [1] G. Pillonnet, H. Fanet and S. Hourri, “Adiabatic capacitive logic: A paradigm for low-power logic,” *2017 IEEE International Symposium on Circuits and Systems (ISCAS)*, pp. 1-4, 2017.
- [2] H. Samaali, Y. Perrin, A. Galisultanov, H. Fanet, G. Pillonnet, et P. Basset, “MEMS four-terminal variable capacitor for low power capacitive adiabatic logic with high logic state differentiation”, *Nano Energy*, vol. 55, p. 277-287, janv. 2019
- [3] Z. A. Ye *et al.*, “Demonstration of 50-mV Digital Integrated Circuits with Microelectromechanical Relays,” *2018 IEEE International Electron Devices Meeting (IEDM)*, pp. 4.1.1-4.1.4, 2018.
- [4] O. Loh and H. D. Espinosa, “Nanoelectromechanical contact switches,” *Nature Nanotechnology*, vol. 7, No. 5, pp. 283-295, 2012.
- [5] C. Pawashe K. Lin, K.J. Kuhn, “Scaling limits of electrostatic nanorelays,” *IEEE Trans. Electron Devices*, vol. 60, pp. 2936–2942, 2013.
- [6] Fanet, Hervé. *Ultra-low power electronics and adiabatic solutions*. John Wiley & Sons, 2016.
- [7] H. Hammer, “Analytical Model for Comb-Capacitance Fringe Fields,” in *Journal of Microelectromechanical Systems*, vol. 19, no. 1, pp. 175-182, Feb. 2010
- [8] Fang, D., Zheng, F., Chen, B. *et al.* “Computation of capacitance and electrostatic forces for the electrostatically driving actuators considering fringe effects”. *Microsyst Technol* **21**, 2089–2096, 2015.

## CONTACT

\*A.Markovic, tel: +33 7 52 98 00 66;

[amarkovic@laas.fr](mailto:amarkovic@laas.fr)